# 1
# Introduction

*Sergey P. Gubin*

## 1.1
## Some Words about Nanoparticles

First of all, it is necessary to consider the general concepts related to the nanosized objects. A nanoobject is a physical object differing appreciably in properties from the corresponding bulk material and having at least 1 nm dimension (not more than 100 nm). When dealing with nanoparticles, magnetic properties (and other physical ones) are size dependent to a large extent. Therefore, particles whose sizes are comparable with (or lesser than) the sizes of magnetic domains in the corresponding bulk materials are the most interesting from a magnetism scientist viewpoint.

Nanotechnology is the technology dealing with both single nanoobjects and materials, and devices based on them, and with processes that take place in the nanometer range. Nanomaterials are those materials whose key physical characteristics are dictated by the nanoobjects they contain. Nanomaterials are classified into compact materials and nanodispersions. The first type includes so-called nanostructured materials [1], i.e., materials isotropic in the macroscopic composition and consisting of contacting nanometer-sized units as repeating structural elements [2]. Unlike nanostructured materials, nanodispersions include a homogeneous dispersion medium (vacuum, gas, liquid, or solid) and nanosized inclusions dispersed in this medium and isolated from each other. The distance between the nanoobjects in these dispersions can vary over broad limits from tens of nanometers to fractions of a nanometer. In the latter case, we are dealing with nanopowders whose grains are separated by thin (often monoatomic) layers of light atoms, which prevent them from agglomeration. Materials containing magnetic nanoparticles, isolated in nonmagnetic matrices at the distances longer than their diameters, are most interesting for magnetic investigations.

A nanoparticle is a quasi-zero-dimensional (0D) nanoobject in which all characteristic linear dimensions are of the same order of magnitude (not more than 100 nm). Nanoparticles can basically differ in their properties from larger

*Magnetic Nanoparticles.* Sergey P. Gubin

ISBN: 978-3-527-40790-3

particles, for example, from long- and well-known ultradispersed powders with a grain size above 0.5 μm. As a rule, nanoparticles are shaped like spheroids. Nanoparticles with a clearly ordered arrangement of atoms (or ions) are called nanocrystallites. Nanoparticles with a clear-cut discrete electronic energy levels are often referred to as ''quantum dots'' or ''artificial atoms''; most often, they have compositions of typical semiconductor materials, but not always. Many magnetic nanoparticles have the same set of electronic levels.

Nanoparticles are of great scientific interest because they represent a bridge between bulk materials and molecules and structures at an atomic level. The term ''cluster,'' which has been widely used in the chemical literature in previous years, is currently used to designate small nanoparticles with sizes less than 1 nm. Magnetic polynuclear coordination compounds (magnetic molecular clusters) belong to the special type of magnetic materials often with unique magnetic characteristics. Unlike nanoparticles, which always have the distributions in sizes, molecular magnetic clusters are the fully identical small magnetic nanoparticles. Their magnetism is usually described in terms of exchange-modified paramagnetism.

Nanorods and nanowires, as shown in Figure 1.1, are quasi-one-dimensional (ID) nanoobjects. In these systems, one dimension exceeds by an order of magnitude the other two dimensions, which are in the nanorange.

The group of two-dimensional objects (2D) includes planar structures – nanodisks, thin-film magnetic structures, magnetic nanoparticle layers, etc., in which two dimensions are an order of magnitude greater than the third one, which is in the nanometer range. The nanoparticles are considered by many authors as giant pseudomolecules having a core and a shell and often also external functional groups. The unique magnetic properties are usually

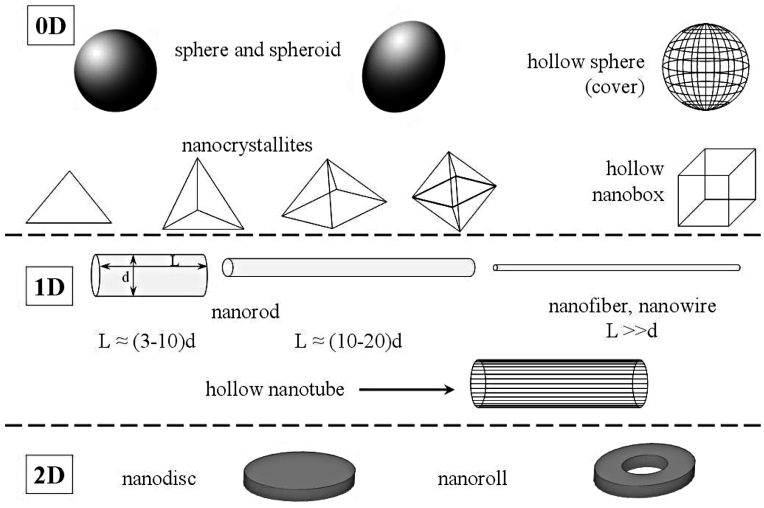


**Figure 1.1** The classification of metal containing nanoparticles by the shape.

inherent in the particles with a core size of 2–30 nm. For magnetic nanoparticles, this value coincides (or less) with the size of a magnetic domain in most bulk magnetic materials. Methods of synthesis and properties of nanoparticles were considered in the books and reports [3].

## 1.2 Scope

Among many of known nanomaterials, the special position belong to those, in which isolated magnetic nanoparticles (magnetic molecular clusters) are divided by dielectric nonmagnetic medium. These nanoparticles present giant magnetic pseudoatoms with the huge overall magnetic moment and ''collective spin.'' In this regard nanoparticles fundamentally differ from the classic magnetic materials with their domain structure. As a result of recent investigations, the new physics of magnetic phenomena – nanomagnetism – was developed. Nanomagnetism advances include superparamagnetism, ultrahigh magnetic anisotropy and coercive force, and giant magnetic resistance. The fundamental achievement of the last time became the development of the solution preparation of the objects with advanced magnetic parameters.

Currently, unique physical properties of nanoparticles are under intensive research [4]. A special place belongs to the magnetic properties in which the difference between a massive (bulk) material and a nanomaterial is especially pronounced. In particular, it was shown that magnetization (per atom) and the magnetic anisotropy of nanoparticles could be much greater than those of a bulk specimen, while differences in the Curie or Néel temperatures between nanoparticle and the corresponding microscopic phases reach hundreds of degrees. The magnetic properties of nanoparticles are determined by many factors, the key of these including the chemical composition, the type and the degree of defectiveness of the crystal lattice, the particle size and shape, the morphology (for structurally inhomogeneous particles), the interaction of the particle with the surrounding matrix and the neighboring particles. By changing the nanoparticle size, shape, composition, and structure, one can control to an extent the magnetic characteristics of the material based on them. However, these factors cannot always be controlled during the synthesis of nanoparticles nearly equal in size and chemical composition; therefore, the properties of nanomaterials of the same type can be markedly different.

In addition, magnetic nanomaterials were found to possess a number of unusual properties – giant magnetoresistance, abnormally high magnetocaloric effect, and so on.

Nanomagnetism usually considers so-called single-domain particles; typical values for the single-domain size range from 15 to 150 nm. However, recently the researchers focused their attention on the particles, whose sizes are smaller than the domain size range; a single particle of size comparable to the minimum domain size would not break up into domains; there is a reason to

call these particles domain free magnetic nanoparticles (DFMN). Each such particle behaves like a giant paramagnetic atom and shows superparamagnetic behavior when the temperature is above the so-called blocking temperature. The experiment shows that the last one can vary in wide diapasons, from few kelvins till higher than room temperature.

Thus, this is a book describing what we need to know to perform nanoscale magnetism – the magnetism of single nanoparticles, well dispersed and isolated one from another. It is important to mention that the intensity of interparticle interactions can dramatically affect the magnetic behavior of their macroscopic ensemble.

Now it became possible to prepare individual nanometer metal or oxide particles not only as ferromagnetic fluids (whose preparation was developed back in the 1960s) [5] but also as single particles covered by ligands or as particles included into ''rigid'' matrices (polymers, zeolites, etc.).

The purpose of this book is to survey the state-of-the-art views on physics, chemistry and methods of preparation and stabilization of magnetic nanoparticles used in nanotechnology for the design of new instruments and devices.

Let us list the most important applications of magnetic nanoparticles: ferrofluids for seals, bearings and dampers in cars and other machines, magnetic recording industry, magnetooptic recording devices, and giant magnetoresistive devices. In recent years, there has been an increasing interest to use magnetic nanoparticles in biomedical applications. Examples of the exciting and broad field of magnetic nanoparticles applications include drug delivery, contrast agents, magnetic hyperthermia, therapeutic *in vivo* applications of magnetic carriers, and *in vitro* magnetic separation and purification, molecular biology investigations, immunomagnetic methods in cell biology and cell separation and in pure medical applications. All of these topics are described to some extent in the following chapters of the book.

### 1.2.1
### Magnetic Nanoparticles Inside Us and Everywhere Around Us

Interstellar space, lunar samples, and meteorites have inclusive magnetic nanoparticles. The geomagnetic navigational aids in all migratory birds, fishes and other animals contain magnetic nanoparticles. The most common iron storage protein ferritin ($[FeOOH]_n$ containing magnetic nanoparticle) is present in almost every cell of plants and animals including humans. The human brain contains over $10^8$ magnetic nanoparticles of magnetite–maghemite per gram of tissue [6]. Denis G. Rancourt has written a nice survey of magnetism of Earth, planetary and environmental nanomaterials [6].

Readers who are interested in more detailed information about the physical properties, magnetic behavior, chemistry, or biomedical applications of magnetic nanoparticles are referred to specific reviews [7].

## 1.3
## The Most Extensively Studied Magnetic Nanoparticles and Their Preparation

A series of general methods for the nanoparticle synthesis have now been developed [8] Most of them can also be used for the preparation of magnetic particles. An essential feature of their synthesis is the preparation of particles of a specified size and shape; at least, the dispersity should be small, 5%–10%, and controllable, since the blocking temperature (and other magnetic characteristics) depends on the particle size. The shape control and the possibility of synthesis of anisotropic magnetic structures are especially important. In order to eliminate (or substantially decrease) the interparticle interactions, magnetic nanoparticles often need to be isolated from one another by immobilization on a substrate surface or in the bulk of a stabilizing matrix or by surfacing with long chain ligands. It is important that the distance between the particles in the matrix should be controllable. Finally, the synthetic procedure should be relatively simple, inexpensive and reproducible.

The development of magnetic materials is often faced with the necessity of preparing nanoparticles of a complex composition, namely, ferrites, FePt, NdFeB or $SmCo_5$ alloys, etc. In these cases, the range of synthetic approaches substantially narrows down. For example, the thermal evaporation of compounds with a complex elemental composition is often accompanied by a violation of the stoichiometery in the vapor phase, resulting in the formation of other substances, while the atomic beam synthesis does not yield a homogeneous distribution of elements in the substrate. The mechanochemical methods of powder dispersion also violate (in some cases, substantially) the phase composition: in particular, ferrites do not retain the homogeneity and oxygen stoichiometery. Furthermore, there is a difficulty of synthesis of the heteroelement precursors required composition. For example, no precursors for $SmCo_5$ with a Sm atom bonded to five Co atoms are known; the maximum chemically attainable element ratio in $Sm[Co(CO)_4]_3$ is 1 : 3. It is even more difficult to propose a stoichiometeric precursor for the synthesis of NdFeB nanoparticles. The overview of general aspects of nanoalloys preparation and characterization and resulting difficulties is presented in [19].

The physical characteristics of nanoparticles are known to be substantially dependent on their dimensions. Unfortunately, most of the currently known methods of synthesis afford nanoparticles with rather broad size distributions (dispersion > 10%). The thorough control of reaction parameters (time, temperature, stirring velocity, and concentrations of reactants and stabilizing ligands) does not always allow one to narrow down this distribution to the required range. Therefore, together with the development of methods for synthesis of nanoparticles with a narrow size distribution, the techniques of separation of nanoparticles into rather monodisperse fractions are perfected. This is done using controlled precipitation of particles from surfactant-stabilized solutions followed by centrifugation. The process is repeated until nanoparticle fractions with specified sizes and dispersion degrees are obtained.

The methods of nanoparticle preparation cannot be detached from stabilization methods. For 1–10 nm particles with a high surface energy, it is difficult to select a really inert medium [10], because the surface of each nanoparticle bears the products of its chemical modification, which affect appreciably the nanomaterial properties. This is especially important for magnetic nanoparticles in which the modified surface layer may possess magnetic characteristics markedly differing from those of the particle core. Nevertheless, the general methods for nanoparticle synthesis are not related directly to the stabilization and the special methods exist where the nanoparticle formation is accompanied by stabilization (in matrices, by encapsulation, etc.).

We do not consider in detail the common methods of magnetic nanoparticles preparation and stabilization. One can find it in the reviews, and partly, in the subsequent chapters of the book.

Among a wide range of the magnetic nanomaterials, nanoparticles of magnetic metals, simple and complex magnetic oxides, and alloys may be separated for detailed analysis.

### 1.3.1 Metals

The metallic nanoparticles have larger magnetization compared to metal oxides, which is interesting for many applications. But metallic magnetic nanoparticles are not air stable, and are easily oxidized, resulting in the change or loss (full or partially) of their magnetization.

#### Fe

Iron is a ferromagnetic material with high magnetic moment density (about 220 emu/g) and is magnetically soft. Iron nanoparticles in the size range below 20 nm are superparamagnetic.

Procedures leading to monodisperse Fe nanoparticles have been well documented [11]. Nevertheless, the preparation of nanoparticles consisting of pure iron is a complicated task, because they often contain oxides, carbides and other impurities. A sample containing pure iron as nanoparticles (10.5 nm) can be obtained by evaporation of the metal in an Ar atmosphere followed by deposition on a substrate [12]. When evaporation took place in a helium atmosphere, the particle size varied in the range of 10–20 nm [13]. Relatively small (100–500 atoms) Fe nanoparticles are formed in the gas phase on laser vaporization of pure iron [14].

The common chemical methods used for the preparations include thermal decomposition of $Fe(CO)_5$ (the particles so prepared are extremely reactive), reductive decomposition of some iron(II) salts, or reduction of iron(III) acetylacetonate; there is a chemical reduction with TOPO capping [15]. A sonochemical method for the synthesis of amorphous iron was developed

in [16]. The method of reducing metal salts by $NaBH_4$ has been widely used to synthesize iron-containing nanoparticles in organic solvents [17]. Normally, reductive synthesis of Fe nanoparticles in an aqueous solution with $NaBH_4$ yields a mixture including FeB [18]. Well-dispersed colloidal iron is required for applications in biological systems such as MRI contrast enhancement and biomaterials separation. Nevertheless, the syntheses have as yet a difficulty in producing stable Fe nanoparticle dispersions, especially aqueous dispersions, for potential biomedical applications.

The phase composition of the obtained nanoparticles was not always determined reliable. The range of specific methods was proposed to prepare nanoparticles of the defined phase composition. Thus, the $\alpha$-Fe nanoparticles with a body-centered cubic (bcc) lattice and an average size of $\sim$10 nm were prepared by grinding a high-purity (99.999%) Fe powder for 32 h [19]. With face-centered cubic (fcc) Fe ($\gamma$-Fe) the situation is more complex. In the phase diagram of a bulk Fe, this phase exists at the ambient pressure in the temperature range of 1183–1663 K, i.e., above the Curie point (1096 K). In some special alloys, this phase, which exhibits antiferromagnetic properties (the Néel temperature is in the 40–67 K range), was observed at room temperature [20]. However, a Mössbauer spectroscopy study [21] has shown that the fcc-Fe nanoparticles (40 nm) remain paramagnetic down to 4.2 K. Some publications dealing with the synthesis of Fe nanoparticles present substantial reasons indicating that these nanoparticles had an fcc structure. Apparently, the nanoparticles containing $\gamma$-Fe were first obtained by Majima *et al.* [22]. These particles contained substantial amounts of carbon (up to 14 mass%) and had an austenite fcc structure analogous to $\gamma$-Fe. However, later, evidence for the existence of the $\gamma$-phase in the Fe nanoparticles that do not contain substantial amounts of carbon has been obtained. Nanoparticles ($\sim$8 nm) consisting, according to powder X-ray diffraction and Mössbauer spectroscopy, of $\gamma$-Fe (30 at.%), $\alpha$-Fe (25 at.%), and iron oxides (45 at.%), were synthesized [23] by treatment of $Fe(CO)_5$ with a $CO_2$ laser. The content of the $\gamma$-phase in the nanoparticles did not change for several years; the particles remained nonmagnetic down to helium temperatures.

Sometimes the determination of phase composition as-synthesized nanoparticles is made difficult. Thus, Fe particles (8.5 nm) were obtained by thermal decomposition of $Fe(CO)_5$ in decalin (460 K) in the presence of surfactants [24]. The X-ray diffraction pattern of the powder formed did not display any sharp maxima, indicating the absence of a crystalline phase. It was assumed that amorphization was due to the high content of carbon ($>$11 mass%) in the nanoparticles studied. Similarly, on ultrasonic treatment of $Fe(CO)_5$ in the gas phase nanoparticles ($\sim$30 nm) were obtained which consisted of $>$96 mass% of Fe, $<$3 mass% of C, and 1 mass% of O [25]. Differential thermal analysis of the powder showed an exothermal transition around 585 K, which corresponded, in the author's opinion, to crystallization of the amorphous iron. As-synthesized particles were pyrophoric due to the large surface area. They were exposed to air which resulted in a thin layer of surface oxidation which also

provides passivation. To prevent the iron nanoparticles from agglomerating, dispersing agents were added during synthesis, as a rule poly(vinylpyrolidone) (PVP). The size dispersion of the nanoparticles produced using physical methods is broader than that in nanoparticles synthesized by chemical methods like reverse micelle, coprecipitation, etc. However, chemical methods yield as a rule only limited quantities of materials.

### Co

Co nanoparticles depending upon the synthetic route are observed in at least three crystallographic phases: typical for bulk Co hcp, $\varepsilon$-Co cubic [26], or multiply twinned fcc-based icosahedral [27]. Conditions of synthesis reactions is influence on the final product structure; in rare cases of the determined phase nanoparticles can be obtained.Often a size and phase selection was required to obtain Co nanocrystals with a specific size and even shape. Methods for the synthesis and magnetic properties of cobalt nanoparticles' different structures have been described in detail in a review [8c].

A popular approach is to synthesize colloidal particles by inversed micelle synthesis; the inverse micelles are defined as a microreactor [28]. In order to obtain stable cobalt nanoparticles with a narrow size distribution, $Co(AOT)_2$ reverse micelles are used; their reduction is obtained by using $NaBH_4$ as a reducing agent. Such particles are stabilized by surfactants and are often monodispersed in size, but are also unstable unless kept in a solution. Nevertheless, the chemical surface treatment by lauric acid highly improves the stability and cobalt nanoparticles could be stored without aggregation or oxidation for at least one week [29] In many instances it is possible to obtain Co nanoparticles coated by other ligands, which can be either dispersed in a solvent or deposited on a substrate; in the latter case, self-organized monolayers having a hexagonal structure can be obtained.

In some instances of reduction with $NaBH_4$ it is possible to obtain Co–B nanoparticles. The size, composition, and structure of this kind of nanoparticles strongly depend on the concentration of the solution, pH, and the mixing procedure [30]. It is well known that the presence of oxides in magnetic materials, which form spontaneously when the metallic surface is in contact with oxygen, drastically changes the magnetic behavior of the particles. An enhanced magnetoresistance, arising from the uniform Co core size and CoO shell thickness, has been reported [31]. This effect is caused by the strong exchange coupling between the ferromagnetic Co core and the antiferromagnetic CoO layer. However, up to now the understanding of this effect has not been well understood.

### Ni

In contrast to cobalt and iron, relatively few reports have been dealing with the physical properties and synthesis of nickel particles. However, the nanosized ferromagnetic Ni is also being widely studied as it presents both

an interest for fundamental sciences and an interest for applications such as magnetic storage, ferrofluids, medical diagnosis, multilayer capacitors, and especially catalysis. Because these properties and applications can be tuned by manipulating the size and structure of the particles, the development of flexible and precise synthetic routes has been an active area of research. A wide variety of techniques have been used to produce nickel nanoparticles: thermal decomposition [32], sol–gel [33], spray pyrolysis [34], sputtering [35], and high-energy ball milling [36]. The organometallic precursors such as $Ni(CO)_4$, $Ni(COD)_2$, and $Ni(Cp)_2$ have also been used for the synthesis and spectroscopic studies of nickel nanoparticles [37, 38]. At present, Ni nanoparticles are generally prepared by microemulsion techniques, using cetyltrimethylammonium bromide (CTAB) [39] or by reduction of Ni ions in the presence of alkyl amines or trioctylphosphine oxide (TOPO) [40]. Some authors showed that the surface of Ni-nanoparticles was readily oxidized to NiO. On the basis of this discovery, they envisioned that the synthesis of large-sized Ni nanoparticles and their subsequent oxidation would provide an NiO shell having high affinity for biomolecules.

### 1.3.2 Nanoparticles of Rare Earth Metals

Six of the nine rare earth elements (REE) are ferromagnetic. The magnetic nanomaterials based on these REE occupy a special place, as they can be used in magnetic cooling systems [41]. However, REE nanoparticles (of both metals and oxides) are still represented by only a few examples, most of all, due to the high chemical activity of highly dispersed REE. A synthesis of coarse (95 × 280 nm) spindle-shaped ferromagnetic EuO nanocrystals suitable for the design of optomagnetic materials has been reported [42]. The EuS nanocrystals were prepared by passing $H_2S$ through a solution of europium in liquid ammonia [43]. The size of the EuS magnetic nanoparticles formed can be controlled (to within 20–36 nm) by varying the amount of pyridine added to the reaction medium [43].

Gadolinium nanoparticles (12 nm) were prepared by reduction of gadolinium chloride by Na metal in THF. They proved to be extremely reactive and pyrophoric, which, however, did not prevent characterization of these particles and measuring their magnetic parameters [44]. The Gd, Dy, and Tb nanoparticles with an average size of 1.5–2.1 nm and an about 20% degree of dispersion were obtained in a titanium matrix by ion beam sputtering [45]. At 4.5 K, the coercive forces for ~10 nm Tb and Gd nanoparticles were 22 and 1 kG, respectively. As the particle size decreases (<10 nm), the Hc value rapidly diminishes to zero, which is related, in the researchers' opinion [46], to the decrease in the Curie temperature for small nanoparticles.

### 1.3.3 Oxidation of Metallic Nanoparticles

Magnetic properties of metallic nanoparticles are dependent on the degree of oxidation of the surface. Therefore, the true knowledge of the degree of nanoparticle oxidation is necessary for the forecasting of magnetic characteristics of the obtained samples. However, as the experiments have shown, it was often difficult. It should be noted that the oxidation of magnetic metal nanoparticles during their synthesis cannot be avoided completely. Thorough mass-spectroscopic analysis of Fe nanoparticles obtained by laser vaporization of the metal in a pure He medium showed that at least 5% of particles contain at least one oxygen atom [47]. If the deposition of oxygen present in the gas phase in trace amounts on the nanoparticle surface cannot be avoided even under these ''exceptional'' conditions, it is evident that under ''usual'' conditions, the nanoparticles of magnetic metals would always contain some amounts of oxides or sub-oxides on the surface. It can be plainly seen in the HRTEM micrograph of Fe nanoparticles (20 nm) synthesized by laser pyrolysis of $Fe(CO)_5$ under inert atmosphere that the particles are coated with a (3.5 nm) layer of iron oxide (the content of the chemically bound oxygen is 14.4 mass%) [48]. At the same time the oxidation of amorphous $Fe_{1-x}C_x$ nanoparticles obtained by thermal decomposition of $Fe(CO)_5$ in decalin in the presence of oleic acid for several weeks in air has shown that the particles (6.9 nm) having a spherical shape and a very narrow size distribution consist of $\alpha$- and $\gamma$-$Fe_2O_3$ [49]. However, passivation of nanocrystalline ($\sim$25 nm) Fe particles obtained by metal evaporation in a helium stream results in only a thin (1–2 nm) film of an antiferromagnetic oxide (apparently, FeO) forming on the surface [50].

The magnetic properties of cobalt nanoparticles, which were obtained by vacuum evaporation on the LiF substrate and then oxidized by exposure to air for a week, have been studied [51]. According to electron diffraction for two samples differing in the particle size (2.3 and 3.0 nm), the intensity of the HCP–Co reflections decreased after oxidation to become $\sim$1/3 of the CoO–HCP line intensity. Hence, a small stable core of unoxidized cobalt remains in all particles after oxidation. Comparative X-ray diffraction studies of the samples consisting of Co nanoparticles distributed in poly-vinylpyridine stored under Ar and in air (the storage time was not indicated) revealed no significant differences [52]. Therefore, the authors considered a low degree of oxidation for cobalt.

In a more comprehensive study [53], $^{57}$Co-enriched cobalt nanoparticles were subjected to oxidation directly in a Mössbauer spectrometer. For this purpose, argon containing $\sim$80 ppm of $O_2$ was passed through the sample at 300 K for 18 h. Analysis of the emission Mössbauer spectra showed that oxidation results in a fairly well-organized CoO layer on the surface of Co particles. Passing pure oxygen through this gently oxidized sample for 1 h at 300 K did not induce any spectral changes; this is indicative of complete

passivation of Co particles at the first oxidation stage. It is thought that such gentle surface oxidation of the Co nanoparticles was always necessary to obtain stable magnetic nanoparticles [54].

In some studies, the preparation of Fe nanoparticles was also followed by their passivation, for example, by keeping for several hours in an atmosphere of oxygen-diluted argon [55]. This procedure prevented further spontaneous particle aggregation. The structure and the magnetic characteristics of such passivated nanoparticles (15–40 nm) have been described in detail [56]. The continuous oxide layers that coat the metallic nanoparticle can be clearly seen in TEM images reported in this study. The interaction of the ferromagnetic core and the oxide shell, which resembles in the magnetic characteristics the interaction of magnetic moments in spin glass, was studied.

The data on the reactivity of Fe nanoparticles with respect to oxidation reported in the literature are contradictory. Thus rather large (~40 nm) nanoparticles of pure Fe obtained by thermal vaporization contained less than 8 mass% of the oxide after exposure to air for three months [57].

In the last few years, for oxidation as-synthesized Fe nanoparticles soft oxidizers such as $(CH_3)_3NO$ were often used.

### 1.3.4 Magnetic Alloys

#### 1.3.4.1 Fe–Co Alloys

It is well known that Co and Fe form a body-centered-cubic solid solution ($Co_xFe_{100-x}$) over an extensive range. The ordered Co–Fe alloys are excellent soft magnetic materials with negligible magnetocrystalline anisotropy [58]. The saturation magnetization of Fe–Co alloys reaches a maximum at a Co content of 35 at.%; other magnetic characteristics of these metals also increase when they are mixed. Therefore, FeCo nanoparticles attract considerable attention. Thus Fe, Co, and Fe–Co (20 at.%, 40 at.%, 60 at.%, 80 at.%) nanoparticles (40–51 nm) with a structure similar to the corresponding bulk phases have been prepared in a stream of hydrogen plasma [59]. The Fe–Co particles reach a maximum saturation magnetization at 40 at.% of Co, and a maximum coercive force is attained at 80 at.% of Co. Chemical reduction by $NaBH_4$ is also used for the preparation of FeCo nanoparticles [60]. X-ray data show that the ratio of Co to Fe is around 30 : 70 in the prepared nanoparticles.

#### Fe-Ni

The bulk samples of the iron–nickel alloys are either nonmagnetic or magnetically soft ferromagnets (for example, permalloys containing >30% of Ni and various doping additives). The Fe–Ni nanoparticles have a much lower saturation magnetization than the corresponding bulk samples over the whole concentration range [61]. An alloy containing

37% of Ni has a low Curie point and an fcc structure. It consists of nanoparticles (12–80 nm) superparamagnetic over a broad temperature range [62]. Theoretical calculations predict a complex magnetic structure for these Fe–Ni particles [63].

**Fe–Pt**

Nanoparticles of this composition have received much attention in recent years due to the prospects for a substantial increase in the information recording density for materials based on them [64]. The face-centered tetragonal (fct) (also known as L10 phase) FePt alloy possesses a very high uniaxial magnetocrystalline anisotropy of ca. $6 \times 10^6$ J/m$^3$, which is more than 10 times as high as that of the currently utilized CoCr-based alloys and, thus, exhibit large coercivity at room temperature, even when their size is as small as several nanometers [65]. These unique properties make them possible candidates for the next generation of magnetic storage media and high-performance permanent magnets [66]. To realize these potentials it is important to develop synthetic methods that yield magnetic nanoparticles of tunable size, shape, dispersity and composition. For these syntheses the most commonly used is the thermal decomposition of organometallic precursors or reduction of metal salts in the presence of long-chain acid or amine and phosphine or phosphine oxide ligands [67]. The as-synthesized FePt nanoparticles possess an fcc structure and are superparamagnetic at room temperature. Thermal annealing converts the fcc FePt to fct FePt (L10), yielding nanocrystalline materials with sufficient coercivity [68]. L10 FePt nanoparticles can be synthesized directly using a polyol reduction method at high temperatures or annealed as-prepared chemically disordered face-centered cubic (fcc) to the chemically ordered L10 phase [69]. There are a number of requirements for such transformations into the L10 phase (except avoiding severe sintering and aggregation): the atomic composition of each nanoparticles should be within 40–60% Fe; the diameter should be larger than the superparamagnetic limit (ca. 3.3 nm); the size distribution should generally be below 10% [70].

The FePt nanoparticles (6 nm) with a narrow size distribution were prepared by joint thermolysis of $Fe(CO)_5$ and $Pt(acac)_2$ in the presence of oleic acid and oleylamine. Further heating resulted in the formation of a protective film from the products of thermal decomposition of the surfactant on the nanoparticle surface, which does not change significantly the particle size. These particles can be arranged to form regular films and so-called colloid crystals. For many practical applications, magnetic nanoparticles larger than 6 nm are preferred because coercivity and the saturation magnetization of the nanoparticles are closely related to the size of magnetic nanoparticles [71]. Later it has been however found that most FePt nanoparticles have the broad composition distribution: approximately 40% and 30% of the nanoparticles were Pt-rich and Fe-rich, respectively. Chemists are in general agreement that to obtain high-quality FePt nanoparticles via this synthetic route and to further

control the size, composition, and size distribution, a better understanding of the reaction mechanism is required. It is believed that the progress in the chemical synthesis of these nanoparticles makes it possible to utilize FePt for large data storage capacities. An excellent review of the synthesis and properties of FePt nanoparticle materials is available [72]. The reaction of FePt nanoparticles with $Fe_3O_4$ followed by heating of the samples at 650 °C in an $Ar + 5\%H_2$ stream resulted in the FePt–$Fe_3Pt$ nanocomposite with unusual magnetic characteristics [73].

#### Co–Pt

The impressive magnetic properties of CoPt nanoparticles according to their size, form, and crystal structure render them as important materials for high-density information storage [74], because they are chemically stable and have very high magnetocrystalline anisotropy $\sim 4 \times 10^6$ J/m$^3$ [75]. A general method applied for the synthesis of CoPt nanoparticles involves the reduction of $Pt(acac)_2$ by 1,2-hexadecanediol, with the simultaneous thermal decomposition of an organometallic cobalt source in dioctyl ether in the presence of oleic acid and oleyl amine [76]. An alternative way to produce metallic nanoparticles avoiding the use of organometallic precursors is the polyol method.

Using the synthesis of $CoPt_3$ nanoparticles as an example, the mechanism of homogeneous nucleation has been studied. It allowed us to deliberately and reproducibly obtain nanoparticles of fixed composition with a narrow size distribution in the 3–18 nm range [77].

The bimetallic particles are not always appropriately termed "alloys." For example, using the same initial compounds, $Co_2(CO)_8$ and $Pt(hfac)_2$, two types of Co–Pt nanoparticles with the same composition and different structures have been obtained [78], namely, particles with a uniform distribution of Co and Pt atoms and particles with a cobalt core and a platinum shell, Pt @ Co. In the latter type of particles, mixing of the atoms of two metals is possible only at the interface. The desired synthesis of such core/shell CoPt nanoparticles has been described [79]. The researchers first obtained Pt nanoparticles of diameter 2.5 nm and then coated them with a controlled amount of Co layers. This resulted in Co–Pt nanoparticles with a diameter of 7.6 nm.

### 1.3.5 Magnetic Oxides

#### Iron Oxides

Iron oxides have received increasing attention due to their extensive applications, such as magnetic recording media, catalysts, pigments, gas sensors, optical devices, and electromagnetic devices [80]. They exist in a rich variety of structures (polymorphs) and hydration states; therefore until recently, knowledge of the structural details, thermodynamics and reactivity of iron oxides

has been lacking. Furthermore, physical (magnetic) and chemical properties commonly change with particle size and degree of hydration. By definition, superparamagnetic iron oxide particles are generally classified with regard to their size into superparamagnetic iron oxide particles (SPIO), displaying hydrodynamic diameters larger than 30 nm, and ultrasmall superparamagnetic iron oxide particles (USPIO), with hydrodynamic diameters smaller than 30 nm. USPIO particles are now efficient contrast agents used to enhance relaxation differences between healthy and pathological tissues, due to their high saturation magnetization, high magnetic susceptibility, and low toxicity. The biodistribution and resulting contrast of these particles are highly dependent on their synthetic route, shape, and size [81]. There has been much interest in the development of synthetic methods to produce high-quality iron oxide systems. The synthesis of controlled size magnetic nanoparticles is described in multiple publications. High-quality iron oxide nanomaterials have been generated using high-temperature solution phase methods similar to those used for semiconductor quantum dots. Other synthesis methods such as polyol-mediated, sol–gel [82] and sonochemical [83] were also proposed. The effectiveness of the nonaqueous routes for the production of well-calibrated iron oxide nanoparticles was shown in [84]. The magnetite nanocrystals (and other) were easily purified using standard methods also developed for quantum dots.

For the variety of magnetic nanomaterials properties the different morphologies including spheres, rods, tubes, wires, belts, cubes, starlike, flowerlike, and other hierarchical architectures were fabricated by various approaches. Finally, some bacteria couple the reduction of Fe(III) with the metabolism of organic materials, which can include anthropogenic contaminants, or simply use iron oxides as electron sinks during respiration [85].

**$Fe_2O_3$**

Among several crystalline modifications of anhydrous ferric oxides there are two magnetic phases, namely, rhombohedral hematite ($\alpha$-$Fe_2O_3$) and cubic maghemite ($\gamma$-$Fe_2O_3$), and the less common $\varepsilon$-$Fe_2O_3$ phases. In the $\alpha$-structure, all $Fe^{3+}$ ions have an octahedral coordination, whereas in $\gamma$-$Fe_2O_3$ having the structure of a cation-deficient $AB_2O_4$ spinel, the metal atoms A and B occur in tetrahedral and octahedral environments, respectively. The oxide $\alpha$-$Fe_2O_3$ is antiferromagnetic at temperatures below 950 K, while above the Morin point (260 K) it exhibits so-called weak ferromagnetism. Hematite, the thermodynamically stable crystallographic phase of iron oxide with a band gap of 2.2 eV, is a very attractive material because of its wide applications, except magnetic recording materials, also in catalysis, as a gas sensors, pigments, and paints. Its nontoxicity is, attractive features for these applications.

The $\alpha$-$Fe_2O_3$ and FeOOH (goethite) nanoparticles are obtained by controlled hydrolysis of $Fe^{3+}$ salts [86]. In order to avoid the formation of other phases, a solution of ammonia is added to a boiling aqueous solution of $Fe(NO_3)_3$ with intensive stirring. After boiling for 2.5 h and treating with ammonium

oxalate (to remove the impurities of other oxides), the precipitate forms a red powder containing $\alpha$-$Fe_2O_3$ nanoparticles (20 nm) [87]. These nanoparticles are also formed on treatment of solutions of iron salts ($Fe^{2+}$: $Fe^{3+} = 1:2$) with an aqueous solution of ammonium hydroxide in air [88]. The synthesis of regularly arranged $\alpha$-$Fe_2O_3$ nanowires with a diameter of 2–5 nm and a length of 20–40 nm has been described [89].

A bulk $\gamma$-$Fe_2O_3$ sample is a ferrimagnet below 620 °C. The $\gamma$-$Fe_2O_3$ nanoparticles (4–16 nm) with a relatively narrow size distribution have been obtained by mild oxidation ($Me_3NO$) of preformed metallic nanoparticles [90]. The same result can be attained by direct introduction of $Fe(CO)_5$ into a heated solution of $Me_3NO$. The oxidation with air is also used to prepare $\gamma$-$Fe_2O_3$ nanoparticles. For this purpose, the $Fe_3O_4$ nanoparticles (9 nm) are boiled in water at pH 12–13 [91]. The kinetics of this process was studied.

The most popular route to $\gamma$-$Fe_2O_3$ nanoparticles is thermal decomposition of $Fe^{3+}$ salts in various media. Rather exotic groups are used in some cases as anions. For example, good results have been obtained by using iron complexes with cupferron [92]. A mechanochemical synthesis of $\gamma$-$Fe_2O_3$ has been described [93]. An iron powder was milled in a planetary mill with water; this is a convenient one-stage synthesis of maghemite nanoparticles (15 nm).

Additionally, nonspherical $Fe_2O_3$ nanoparticals, such as nanorods, nanowires, nanobelts, and nanotubes, have also been synthesized and used for investigating their peculiar magnetic properties [94].

**$Fe_3O_4$ (Magnetite)**

Among all iron oxides, magnetite $Fe_3O_4$ possess the most interesting properties because of the presence of iron cations in two valence states, $Fe^{2+}$ and $Fe^{3+}$, in the inverse spinel structure. The cubic spinel $Fe_3O_4$ is ferrimagnetic at temperatures below 858 K. The route to these particles used most often involves treatment of a solution of a mixture of iron salts ($Fe^{2+}$ and $Fe^{3+}$) with a base under an inert atmosphere. For example, the addition of an aqueous solution of ammonia to a solution of $FeCl_2$ and $FeCl_3$ (1 : 2) yields nanoparticles, which are transferred into a hexane solution by treatment with oleic acid [95]. The repeated selective precipitation gives $Fe_3O_4$ nanoparticles with a rather narrow size distribution. The synthesis can be performed starting only from $FeCl_2$, but in this case, a specified amount of an oxidant ($NaNO_2$) should be added to the aqueous solution apart from alkali. This method allows one to vary both the particle size (6.5–38 nm) and (to a certain extent) the particle shape [96].

In some cases, thermal decomposition of compounds containing $Fe^{3+}$ ions under oxygen-deficient conditions is accompanied by partial reduction of $Fe^{3+}$ to $Fe^{2+}$. Thus thermolysis of $Fe(acac)_3$ in diphenyl ether in the presence of small amounts of hexadecane-l,2-diol (probable reducer of a part of $Fe^{3+}$ ions to $Fe^{2+}$) gives very fine $Fe_3O_4$ nanoparticles (about 1 nm), which can be enlarged by adding excess $Fe(acac)_3$ into the reaction mixture [97]. $Fe_3O_4$

nanoparticles can be also prepared in uniform sizes of about 9 nm by autoclave heating the mixture, consisting of $FeCl_3$, ethylene glycol, sodium acetate, and polyethylene glycol [98]. For partial reduction of $Fe^{3+}$ ions, hydrazine has also been recommended [99]. The reaction of $Fe(acac)_3$ with hydrazine is carried out in the presence of a surfactant. This procedure resulted in superparamagnetic magnetite nanoparticles with controlled sizes, 8 and 11 nm.

The so-called dry methods are used alongside with the solution ones. Thus, $Fe_3O_4$ nanoparticles with an average size of 3.5 nm have been prepared by thermal decomposition of $Fe_2(C_2O_4)_3 \cdot 5H_2O$ at $T > 400\,^{\circ}C$ [100]. Furthermore, the controlled reduction of ultradispersed $\alpha$-$Fe_2O_3$ in a hydrogen stream at 723 K (15 min) is a more reliable method of synthesis of $Fe_3O_4$ nanoparticles. Particles with ~13 nm size were prepared in this way [101].

The stabilization in the water media is interesting for bioapplications, but at the same time a problem also. For solving it cyclodextrin was used to transfer obtained organic ligand stabilized iron oxide nanoparticles to aqueous phase via forming an inclusion complex between surface-bound surfactants and cyclodextrin [102].

In contrast, higher nanoparticles (20 nm $< d <$ 100 nm) are of great interest, mainly for hyperthermia because of their ferrimagnetic behavior at room temperature. However, there are some difficulties encountered when obtaining a monodisperse magnetite particle of size larger than 20 nm and controlling the stoichiometery.

**Ferrites**

Microcrystalline ferrites form the basis of materials currently used for magnetic information recording and storage. To increase the recorded information density, it seems reasonable to obtain nanocrystalline ferrites and to prepare magnetic carriers based on them. Grinding of microcrystalline ferrite powders to reach the nanosize of grains is inefficient, as this gives particles with a broad size distribution, the content of the fraction with the optimal particle size (30–50 nm) being relatively low.

The key method for the preparation of powders of magnetic hexagonal ferrites with a grain size of more than 1 μm includes heating of a mixture of the starting compounds at temperature above 1000 °C (so-called ceramic method). An attempt has been made to use this method for the synthesis of barium ferrite nanoparticles [103]. The initial components (barium carbonate and iron oxide) were ground for 48 h in a ball mill and the resulting powder was mixed for 1 h at a temperature somewhat below 1000 °C. This gave rather large particles (200 nm and greater) with a broad size distribution. Similar results have been obtained in the mechanochemical synthesis of barium ferrite [104].

Nanocrystalline ferrites are often prepared by the coprecipitation method. The $MnFe_2O_4$ spinel nanoparticles with a diameter of 40 nm are formed upon the addition of an aqueous solution of stoichiometeric amounts of $Mn^{2+}$ and $Fe^{3+}$ chlorides to a vigorously stirred solution of alkali

[105]. The $MgFe_2O_4$ (6–18 nm) nanoparticles were obtained in a similar way. In contrast, the $SrFe_{12}O_{19}$ nanoparticles (30–80 nm) were synthesized by coprecipitation of Sr and Fe citrates followed by annealing of the resulting precipitate [106]. Coprecipitation upon decomposition of a mixture of $Fe(CO)_5$ and $Ba(O_2C_7H_{15})_2$ under ultrasonic treatment has been successfully used for the synthesis of barium ferrite nanoparticles (~50 nm) [107].

Methods for the preparation of ferrite nanoparticles of different compositions in solutions at moderate temperatures have been developed. First, worth mentioning is the sol–gel method resulting in highly dispersed powders with required purity and homogeneity. Low annealing temperatures allow one to control crystallization and to obtain single-domain magnetic ferrite nanoparticles with narrow size distributions and to easily dope the resulting particles with metal ions. This procedure was used to obtain Co- and Ti-doped barium ferrite nanoparticles (smaller than 100 nm) and, Zn-, Ti-, and Ir-doped strontium ferrite particles with a similar size [108].

Smaller nanoparticles (15–25 nm) of cobalt ferrite were obtained in a hydrogel containing lecithin as the major component. Judging by the good magnetic characteristics, these particles possessed a substantial degree of crystallinity without any annealing [109]. The sol–gel method was successfully used to synthesize a Co ferrite nanowire 40 nm in diameter with a length of up to a micrometer [110]. This wire can also be obtained within carbon nanotubes [111]. For the synthesis of ferrite nanoparticles, oil-in-water type micelles [112] and reverse (water-in-oil) micelles [113] are also widely used.

The homogeneity of metal ion distribution in final products can be enhanced, and the required stoichiometry can be attained by using presynthesis of heterometallic complexes of various composition. The thermal decomposition and annealing of the presynthesized $[GdFe(OPr')_6(HOPr')]_2$ complex give $GdFeO_4$ nanoparticles (~60 nm) [114]. It is also pertinent to consider the procedure for the synthesis of cobalt ferrite $CoFe_2O_4$ nanoparticles, in which the first stage includes the preparation of the Fe–Co heterometallic particles and the second stage, their oxidation to $CoFe_2O_4$ [115]. Another route to analogous particle implies the use the heterometallic $(\eta^5\text{-}C_5H_5)CoFe_2(CO)_9$ cluster as the starting compound. The cobalt ferrite nanoparticles were also prepared by the microemulsion method from a mixture of Co and Fe dodecylsulfates treated with an aqueous solution of methylamine [116].

**FeO (Wustite)**

Cubic $Fe^{2+}$ oxide is antiferromagnetic ($T_c = 185$ K) in the bulk state. Joint milling of Fe and $Fe_2O_3$ powders taken in a definite ratio give nanoparticles (5–10 nm) consisting of FeO and Fe [117]. On heating these particles at temperatures of 250–400 °C, the metastable FeO phase disproportionates to $Fe_3O_4$ and Fe, while above 550 °C it is again converted into nanocrystalline FeO [118].

### FeOOH

The oxyhydroxides, nominally FeOOH, include goethite, lepidocrocite, akaganeite, and several other polymorphs. They often contain excess water. Ferrihydrite $Fe_5HO_8{\cdot}4(H_2O)$ is typically considered a metastable iron oxide that can act as a precursor to the more stable iron oxides such as goethite and hematite [119]. Oxyhydroxides are normally obtained by precipitation from an aqueous solution. The particle size is controlled by initial iron concentration, organic additives, pH, and temperature.

### $\alpha$-FeOOH (Goethite)

Among the known oxide hydroxides $Fe_2O_3{\cdot}H_2O$, the orthorhombic $\alpha$-FeOOH (goethite) is antiferromagnetic in the bulk state and has $T_c = 393$ K [120]. Synthetic goethite nanoparticles are typically acicular and are often aggregated into bundles or rafts of oriented crystallites. $\beta$-FeOOH (akagenite) is paramagnetic at 300 K [121]. Akaganeite always has a significant surface area and some amount of excess water, which increases tremendously with the decreasing particle size. Recent studies of nanoakaganite show that at very high surface areas, where the particle size becomes comparable to a few unit cells, akaganeite may contain goethite-like structural features possibly related to the collapse of exposed tunnels.

$\gamma$-FeOOH (lipidocrokite) is paramagnetic at 300 K and $\delta$-FeOOH (ferroxyhite) is ferromagnetic [122]. Although the bulk $\alpha$-FeOOH is antiferromagnetic, in the form of nanoparticles it has a nonzero magnetic moment due to the incomplete compensation of the magnetic moments of the sublattices. Goethite nanoparticles have been studied by Mössbauer spectroscopy [123]. As a rule, $\alpha$-FeOOH is present in iron nanoparticles as an admixture phase. Ferrihydrite is widespread but the nature of its extensive disorder is still controversial Because of chemical and structural variability in FeOOH containing nanoparticles, it is also critical to determine their chemical composition, including water content, surface area, and particle size.

### Co oxides

Cubic cobalt oxide is antiferromagnetic and has $T_N = 291$ K. Cobalt monoxide has played an important role in the discovery of the ''exchange shift'' of the hysteresis curve, first found for samples consisting of oxidized Co nanoparticles [124]. Data on the dependence of $T_N$ on the particle size were obtained in a study of CoO nanoparticles dispersed in a LiF matrix [125]. The particles obtained by vacuum deposition contained a small metal core, according to powder X-ray diffraction. As the particle size decreased from 3 to 2 nm, $T_N$ decreased from 170 to 55 K. Apparently, the presence of an oxide layer on cobalt nanoparticles can markedly increase the coercive force. For example, the coercive forces (at 5 K) of monodisperse 6 and 13 nm oxidized Co particles obtained by plasma gas condensation in an installation for the investigation of molecular beams were $\sim$5 and 2.4 kG, respectively [126].

Unfortunately, the blocking temperature for 6 nm nanoparticles was lower than room temperature (~200 K); therefore, under normal conditions, their coercive force was equal to zero.

#### $Co_3O_4$

The $Co_3O_4$ nanoparticles (cubic spinel) with sizes of 15–19 nm dispersed in an amorphous silicon matrix exhibited ferrimagnetic properties at temperatures below 33 K (for bulk samples, $T_N = 30$ K) [127]. A method for controlled synthesis of $Co_3O_4$ cubic nanocrystallites (10–100 nm) has been developed [128].

#### NiO

Bulk crystals of NiO are antiferromagnetic, the Néel temperature being 523 K, but when the nanoparticles sizes are of the order of a few nanometers, they become superparamagnetic or superantiferromagnetic [129]. NiO possess not only magnetic but also electrical properties. The conductivity increases by 6–8 orders of magnitude in nanosized NiO as compared to that of bulk crystals, something that is attributed to the high density of defects [130]. It has been pointed out that electrodes composed of NiO nanoparticles exhibit a higher capacity and better cyclability than the ordinary ceramic material [131].

### 1.3.6 Final Remarks

We discussed above ''free'' nanoparticles as powders or suspensions in liquid media. In practice, magnetic nanoparticles are normally used as films (2D systems) or compact materials (3D systems). The compacting of magnetic nanoparticles even those having a protective coating on the surface often results in the loss of or substantial change in their unique physical (magnetic) characteristics. If the nanosized magnetic particles are retained after compaction, the materials based on them can serve as excellent initial components for the preparation of permanent magnets. A highly promising method of stabilization is the introduction of nanoparticles in different types of matrices. An optimal material should be a nonmagnetic dielectric matrix with single-domain magnetic nanoparticles with a narrow size distribution regularly arranged in the matrix. Various organic polymers are mostly used as these matrices. Encapsulation of magnetic nanoparticles makes them stable against oxidation, corrosion and spontaneous aggregation, which allows them to retain the single-domain structure. The magnetic particles coated by a protective shell or introduced in matrix can find application as the information recording media, for example, as magnetic toners in xerography, magnetic ink, contrasting agents for magnetic resonance images, ferrofluids and so on. The appropriate material has been given adequate consideration in the subsequent chapters.

## References


1. P. Moriarty, *Rep. Prog. Phys.*, **2001**, *64*, 297.
2. A.I. Gusev, A.A. Rampel, *Nanokristallicheskie Materialy (Nanocrystalline Materials)*, Moscow: Fizmatlit, **2001**.
3. (a) A.P. Alivisatos, P.F. Barbara, A.W. Castleman, J. Chang, D.A. Dixon, M.L. Klein, G.L. McLendon, J.S. Miller, M.A. Ratner, P.J. Rossky, S.I. Stupp, M.E. Thompson, *Adv. Mater.*, **1998**, *10*, 1297; (b) T. Sugimoto, *Monodispersed Particles*, Elsevier, **2001**; (c) *"Nanostructured Materials; Selected Synthesis, Methods, Properties and Applications,"* Eds., P. Knauth and J. Schoonman, Kluwer, Dordrecht, **2004**; (d) J.P. Wilcoxon, B.L. Abrams, *Chem. Soc. Rev.*, **2006**, *35*, 1162; O. Masala, R. Sesadri, *Ann. Rev. Mater. Res.*, **2004**, *34*, 41.
4. (a) J.-T. Lue, *J. Phys. Chem. Solids.* **2001**, *62*, 1599; (b) J. Jortner, C.N.R. Rao, *Pure Appl. Chem.*, **2002**, *74*, 1491; (c) N.L. Rosi, C.A. Mirkin, *Chem. Rev.*, **2005**, *105*, 1547.
5. (a) V.E. Fertman, *Magnetic Fluids Guide-Book: Properties and Application*, Hemisphere, New York, **1990**; (b) B.M. Berkovsky, V.F. Medvedev, M.S. Krakov, *Magnetic Fluides: Engineering Applications*, Oxford University Press, Oxford, **1993**.
6. J.L. Kirschvink, A. Kirschvink-Kobayashi, B.J. Woodford, *Proc. Natl. Acad. Sci*, **1992**, *89*, 7683.
7. D.G. Rancourt, *Rev. Mineral. Geochem.*, **2001**, *44*, 217.
8. (a) S.P. Gubin, Yu.A. Koksharov, G.B. Khomutov, G.Yu. Yurkov, *Russian Chem. Rev.*, **2005**, *74*, 489; (b) An-Hui-Lu, E.L. Salabas, F. Schuth, *Angew. Chem. Int. Ed.*, **2007**, *46*, 1222; (c) S.P. Gubin, Yu.A. Koksharov, *Neorg. Mater.*, **2002**, *38*, 1287.
9. R. Ferrando, J. Jellinek, R.L. Johnston, *Chem. Rev,*, **2008**, *108*, 845.
10. S.P. Gubin, *Ros. Khim. Zh.*, **2000**, *44*(6), 23.
11. (a) W.J Zhang, *Nanopart. Res.*, **2003**, *5*, 323; (b) D.L. Huber, *Small* **2005**, *1*, 482.
12. S. Gangopadhyay, G.C. Hadjipanayis, B. Dale, C.M. Sorensen, K.J. Klabunde, V. Papaefthymiou, A. Kostikas, *Phys. Rev.*, **1992**, *B 45*, 9778.
13. J.F. Loffler, J.P. Meier, B. Doudin, J.-P. Ansermet, W. Wagner, *Phys. Rev.*, **1998**, *B 57*, 2915.
14. W.A. de Heer, P. Milani, A. Chatelain, *Phys. Rev. Lett.*, **1990**, *65*, 488.
15. L. Guo, Q.J. Huang, X.Y. Li, S.H. Yang. *Phys. Chem. Chem. Phys.* **2001**, *3*, 1661.
16. K.S. Suslick, C. Seok-burn, A.A. Cichowlas, M.W. Grinstaff, *Nature* **1996**, *353*, 414.
17. S.M. Ponder, J.G. Darab, J. Bucher, D. Caulder, I. Craig, L. Davis, N. Edelstein, W. Lukens, H. Nitsche, L. Rao, D.K. Shuh, T.E. Mallouk, *Chem. Mater.*, **2001**, *13*, 479.
18. A.S. Dehlinger, J.F. Pierson, A. Roman, P.H. Bauer, *Surf. Coat. Technol.*, **2003**, *174*, 331.
19. L. Del Bianco, A. Hernando, E. Bonetti, E. Navarro, *Phys. Rev.*, **1997**, *B 56*, 8894.
20. U. Gonser, H.G. Wagner, *Hyperfine Interact.*, **1985**, *24–26*, 769.
21. N. Saegusa, M. Kusunoki, *Jpn. J. Appl. Phys.*, **1990**, *29*, 876.
22. T. Majima, T. Ishii, Y. Matsumoto, M. Takami, *J. Am. Chem. Soc.*, **1989**, *111*, 2417.
23. K. Haneda, Z.X. Zhou, A.H. Morrish, T. Majima, T. Miyahara, *Phys. Rev.*, **1992**, *B46*, 13832.
24. J. van Wonterghem, S. Morup, S.W. Charles, S. Wells, J. Villadsen, *Phys. Rev. Lett.*, **1985**, *55*, 410.
25. M.W. Grinstaff, M.B. Salamon, K.S. Suslick, *Phys. Rev.*, **1993**, *B48*, 269.
26. D.P. Dinega, M.G. Bawendi, *Angew. Chem. Int. Ed. Engl.* **1999**, *38*, 1788.
27. O. Kitakami *et al..*, *Phys. Rev.*, **1997**, *B 56*, 849.
28. M. Pileni, *Appl. Surf. Sci.*, **2001**, *171*, 1.

29. M.P. Pileni, *Langmuir*, **1997**, *13*, 3266.
30. L. Yiping, G.C. Hadjipanayis, V. Papaefthymiou, A. Kostikas, A. Simopoulos, C.M. Sorensen, K.J. Klabunde, *J. Magn. Magn. Mater.*, **1996**, *164*, 357.
31. D.L. Peng, K. Sumiyama, T.J. Konno, T. Hihara, and S. Yamamuro, *Phys. Rev.*, **1999**, *B 60*, 2093.
32. L. Bi, S. Li, Y. Zhang, D. Youvei, *J. Magn. Magn. Mater.* **2004**, *277*, 363.
33. O. Cıntora-Gonzalez, C. Estournes, M. Richard Pionet, J.L. Guille, *Mater. Sci. Eng., C* **2001**, *15*, 179.
34. W.N. Wang, I. Yoshifimi, I. Wuled-Lengorro, K. Okuyama, *Mater Sci. Eng., B* **2004**, *111*, 69.
35. A. Gavirin, C.L. Chen, *J. Appl. Phys.*, **1993**, *73*, 6949.
36. S. Doppiu, V. Langlais, J. Sort, S. Surinach, M.D. Baro', Y. Zhang, G. Hadjinapayis, J. Nogue's, *Chem. Mater.*, **2004**, *16*, 5664.
37. C. Estourne's, T. Lutz, J. Happich, T. Quaranta, P. Wissler, J.L. Guille, *J. Magn. Magn. Mater.*, **1997**, *173*, 83.
38. D. de Caro, J.S. Bradley, *Langmuir*, **1997**, *13*, 3067.
39. D.-H. Chen, S.-H. Wu, *Chem. Mater.*, **2000**, *12*, 1354.
40. K.L. Tsai, J. Dye., *Chem. Mater.*, **1993**, *5*, 540.
41. A.M. Tishin, Yu.I. Spichkin, *The Magnetocaloric Effect and Its Applications*, Institute of Physics: Bristol, Philadelphia, **2003**.
42. S. Thongchant, Y. Hasegawa, Y. Wada, S. Yanagia, *Chem. Lett.*, **2001**, *30*, 1274.
43. S. Thongchant, Y. Hasegawa, Y. Wada, S. Yanagida, *Chem. Lett.*, **2003**, *32*, 706.
44. J.A. Nelson, L.H. Bennet, M.J. Wagner, *J. Am. Chem. Soc.*, **2002**, *124*, 2979.
45. D. Johnson, P. Perera, M.J. O'Shea, *J. Appl. Phys., 79*, 5299.
46. M.J. O'Shea, P. Perera, *J. Appl. Phys.*, **1999**, *85*, 4322.
47. W.A. de Heer, P. Milani, A. Chatelain, *Phys. Rev. Lett.* **1990**, *65*, 488.
48. X.Q. Zhao, Y. Liang, Z.Q. Hu, B.X. Liu, *J. Appl. Phys.*, **1996**, *80*, 5857.
49. M.D. Bentzon, J. van Wonterghem, S. Morup, A. Tholen, C.J.W. Koch, *Philos. Mag.*, **1989**, *B 60*, 169.
50. C. Prados, M. Multigner, A. Hernando, J.C. Sanchez, A. Fernandez, C.F. Conde, A. Conde, *J. Appl. Phys.*, **1999**, *85*, 6118.
51. S. Sako, K. Ohshima, M. Sakai, S. Bandow, *Surf. Rev. Lett.*, **1996**, *3*, 109.
52. M. Respaud, J.M. Broto, H. Rakoto, A.R. Fert, L. Thomas, B. Barbara, M. Verelst, E. Snoeck, P. Lecante, A. Mosset, J. Osuna, T. Ould Ely, C. Amiens, B. Chaudret, *Phys. Rev.*, **1998**, *B 57*, 2925.
53. F. Bodker, S. Morup, S.W. Charles, S. Linderoth, *J. Magn. Magn. Mater.*, **1999**, *196–197*, 18.
54. H. Bonneman, W. Brijoux, R. Brinkmann, N. Matoussevitch, N. Waldoefner, N. Palina, H. Modrow, *Inorg. Chim. Acta*, **2003**, *350*, 617.
55. S. Gangopadhyay, G.C. Hadjipanayis, B. Dale, C.M. Sorensen, K.J. Klabunde, V. Papaefthymiou, A. Kostikas, *Phys. Rev.*, **1992**, *B 45*, 9778.
56. L. Del Bianco, A. Hernando, M. Multigner, C. Prados, J.C. Sanchez-Lopez, A. Fernandez, C.F. Conde, A. Conde, *J. Appl. Phys.*, **1998**, *84*, 2189.
57. H.Y. Bai, J.L. Luo, D. Jin, J.R. Sun, *J. Appl. Phys.*, **1996**, *79*, 361.
58. T. Sourmail, *Prog. Mater. Sci.*, **2005**, *50*, 816.
59. X.G. Li, T. Murai, T. Saito, S. Takahashi, *J. Magn. Magn. Mater.*, **1998**, *190*, 277.
60. B.L. Cushing, V.L. Kolesnichenko, C.J. O'Connor, *Chem. Rev.*, **2004**, *104*, 3893.
61. X.G. Li, A. Chiba, S. Takahashi, *J. Magn. Magn. Mater.*, **1997**, *170*, 339.
62. A.M. Afanas'ev, I.P. Suzdalev, M.Ya. Gen, V.I. Gol'danskii, V.P. Korneev, E.A. Manykin, *Zh. Eksp. Teor. Fiz.*, **1970**, *58*, 115.

63. B.K. Rao, S.R. de Debiaggi, P. Jena, *Phys. Rev.*, **2001**, *B 64*, 418.
64. S. Sun, H. Zeng, *J. Am. Chem. Soc.*, **2002**, *124*, 8204.
65. S. Sun, E.E. Fullerton, D. Weller, C.B. Murray, *IEEE Trans. Magn.*, **2001**, *37*, 1239.
66. T. Hyeon, *Chem. Commun.*, **2003** 927.
67. M. Chen, J.P. Liu, S. Sun, *J. Am. Chem. Soc.*, **2004**, *126*, 8394.
68. K. Elkins, D. Li, N. Poudyal, V. Nandwana, Z. Jin, K. Chen, J.P. Liu, *J. Phys. D: Appl. Phys.*, **2005**, *38*, 2306.
69. H. Kodama, S. Momose, T. Sugimoto, T. Uzumaki, A. Tanaka, *IEEE Trans. Mag.*, **2005**, *41*, 665.
70. B. Stahl, J. Ellrich, R. Theissmann, M. Ghafari, S. Bhattacharya, H. Hahn, N.S. Gajbhiye, D. Kramer, R.N. Viswanath, J. Weissmuller, H. Gleiter, *Phys. Rev. B* **2003**, *67*, 14422.
71. R.C. O'Handley, *Modern Magnetic Materials: Principle and Applications*, Wiley-Interscience: New York 434, **2000**.
72. S. Sun, *Adv. Mater.* **2006**, *18*, 393.
73. H. Zeng, J. Li, J.P. Liu, Z.L. Wang, S. Sun, *Nature*, **2002**, *420*, 395.
74. B. Warne, O.I. Kasyutich, E.L. Mayes, J.A.L. Wiggins, K.K.W. Wong, *IEEE Trans. Magn*, **2000**, *36*, 3009.
75. D. Weller, M.F. Doerner, *Annu. Rev. Mater. Sci.*, **2000**, *30*, 611.
76. S. Sun, C.B. Murray, D. Weller, L. Folks, A. Moser, *Science* **2000**, *287*, 1989.
77. E.V. Shevchenko, D.V. Talapin, H. Schnablegger, A. Kornowski, O. Festin, P. Svedlindh, M. Haase, H. Weller, *J. Am. Chem. Soc.*, **2003**, *125*, 9090.
78. J.-I. Park, J. Cheon, *J. Am. Chem. Soc.*, **2001**, *123*, 5743.
79. N.S. Sobal, U. Ebels, H. Mohwald, M. Giersig, *J. Phys. Chem.*, **2003**, *B 107*, 7351.
80. R.M. Cornell, U. Schwertmann, *The Iron Oxides: Structure, Properties, Reactions, Occurrences and Uses*, 2nd ed.; Wiley-VCH: Weinheim, **2003**.
81. P. Tartaj, M.P. Morales, S. Veintemillas-Verdaguer, T. Gonzalez-Carren, C.J. Serna, *J. Magn. Magn. Mater.* **2005**, *290–291*, 28.
82. C. Feldmann, H.-O. Jungk, *Angew. Chem., Int. Ed.* **2001**, *40*, 359.
83. R. Vijaya Kumar, Yu. Koltypin, Y.S. Cohen, Y. Cohen, D. Aurbach, O. Palchik, I. Felner, A. Gedanken, *J. Mater. Chem.* **2000**, *10*, 1125.
84. Z. Li, H. Chen, H. Bao, M. Gao, *Chem. Mater.* **2004**, *16*, 1391.
85. D.R. Lovley, *Microbiol. Rev.* **1991**, *55*, 259.
86. U. Schwertmann, E. Murad, *Clays Clay Miner.*, **1983**, *31*, 277.
87. M.F. Hansen, C.B. Koch, S. Morup, *Phys. Rev.*, **2000**, *B 62*, 1124.
88. L. Zhang, G.C. Papaefthymiou, J.Y. Ying, *J. Appl. Phys.*, **1997**, *81*, 6892.
89. Y.Y. Fu, R.M. Wang, J. Xu, J. Chen, Y. Yan, A.V. Narlikar, H. Zhang, *Chem. Phys. Lett.*, **2003**, *379*, 373.
90. T. Hyeon, S.S. Lee, J. Park, Y. Chung, H.B. Na, *J. Am. Chem. Soc.*, **2001**, *123*, 12798.
91. J. Tang, M. Myers, K.A. Bosnick, L.E. Brus, *J. Phys. Chem.*, **2003**, *B 107*, 7501.
92. J. Rockenberger, E.C. Scher, A.P. Alivisatos, *J. Am. Chem. Soc.*, **1999**, *121*, 11595.
93. R. Janot, D. Guerard, *J. Alloys Compd.*, **2002**, *333*, 302.
94. (a) Z. Jing, S. Wu, *Mater. Lett.*, **2004**, *58*, 3637; (b) X.G. Wen, S.H. Wang, Y. Ding, Z.L. Wang, S.H. Yang, *J. Phys.Chem. B*, **2005**, *109*, 215.
95. T. Fried, G. Shemer, G. Markovich, *Adv. Mater.*, **2001**, *13*, 1158.
96. I. Nedkov, T. Merodiiska, S. Kolev, K. Krezhov, D. Niarchos, E. Moraitakis, Y. Kusano, J. Takada, *Monatsh. Chem.*, **2002**, *133*, 823.
97. S. Sun, H. Zeng, *J. Am. Chem. Soc.*, **2002**, *124*, 8204.
98. X. Wang, J. Zhuang, O. Peng, Y. Li, *Nature*, **2005**, *437*, 121.
99. Y. Hou, J. Yu, S. Gao, *J. Mater. Chem.*, **2003**, *13*, 1983.
100. Yu.F. Krupyanskii, I.P. Suzdalev, *Zh. Eksp. Teor. Fiz.*, **1974**, *67*, 736.
101. R.N. Panda, N.S. Gajbhiye, G. Balaji, *J. Alloys Compd.*, **2001**, *326*, 50.

102. W.W. Yu, X. Peng, *Angew. Chem. Int. Edn.*, **2002**, *41*, 2368.
103. G. Benito, M.P. Morales, J. Requena, V. Raposo, M. Vazquez, J.S. Moya, *J. Magn. Magn. Mater*, **2001**, *234*, 65.
104. J. Ding, T. Tsuzuki, P.G. McCormick, *J. Magn. Magn. Mater.*, **1998**, *177–181*, 931.
105. Z.J. Zhang, Z.L. Wang, B.C. Chakoumakos, J.S. Yin, *J. Am. Chem. Soc.*, **1998**, *120*, 1800.
106. A. Vijayalakshimi, N.S. Gajbhiye, *J. Appl. Phys.*, **1998**, *83*, 400.
107. K.V.P.M. Shafi, A. Gedanken, *Nanostruct. Mater.*, **1999**, *12*, 29.
108. G. Mendoza-Suarez, J.C. Corral-Huacuz, M.E. Contreras-Garcia, H. Juarez-Medina, *J. Magn. Magn. Mater.*, **2001**, *234*, 73.
109. S. Li, V.T. John, S.H. Rachakonda, G.C. Irvin, G.L. McPherson, C.J. O'Connor, *J. Appl. Phys.*, **1999**, *85*, 5178.
110. G. Ji, S. Tang, B. Xu, B. Gu, Y. Du, *Chem. Phys. Lett.*, **2003**, *379*, 484.
111. C. Pham-Huu, N. Keller, C. Estournes, G. Ehret, J.M. Greneche, M.J. Ledoux, *Phys. Chem. Chem. Phys.*, **2003**, *5*, 3716.
112. C. Liu, A.J. Rondinone, Z.J. Zhang, *Pure Appl. Chem.*, **2000**, *72*, 37.
113. C.J. O'Connor, Y.S.L. Buisson, S. Li, S. Banerjee, R. Premchandran, T. Baumgartner, V.T. John, G.L. McPherson, J.A. Akkara, D.L. Kaplan, *J. Appl. Phys.*, **1997**, *81*, 4741.
114. S. Mathur, H. Shen, N. Lecerf, A. Kjekshus, H. Fjellvag, G.F. Goya, *Adv. Mater.*, **2002**, *14*, 1405.
115. T. Hyeon, Y. Chung, J. Park, S.S. Lee, Y.W Kim, B.H. Park, *J. Phys. Chem.*, **2002**, *B 106*, 6831.
116. N. Moumen, M.P. Pileni, *Chem. Mater.*, **1996**, *8*, 1128.
117. J. Ding, W.F. Miao, E. Pirault, R. Street, P.G. McCormick, *J Alloys Compd.*, **1998**, *161*, 199.
118. (a) L. Minervini, R.W. Grimes, *J. Phys. Chem. Solids*, **1999**, *60*, 235; (b) K. Tokumitsu, T. Nasu, *Scr. Metall.*, **2001**, *44*, 1421.
119. U. Schwertmann, J. Friedl, H. Stanjek, D.G. Schulze, *Clay Miner.* **2000**, *35*, 613.
120. C.J.W. Koch, M.B. Madsen, S. Morup, *Hyperfine Interact.*, **1986**, *28*, 549.
121. S. Morup, T.M. Meaz, C.B. Koch, H.C.B. Hansen, *Z. Phys.*, **1997**, *D 40*, 167.
122. T. Meaz, C.B. Koch, S. Morup, in *Proceedings of the Conference ICAME-95, Bologna*, **1996**, *50*, 525.
123. M.B. Madsen, S. Morup, *Hyperfine Interact.*, **1988**, *42*, 1059.
124. M. Kiwi, *J. Magn. Magn. Mater.*, **2001**, *234*, 584.
125. S. Sako, K. Ohshima, M. Sakai, S. Bandow, *Surf. Rev. Lett.*, **1996**, *3*, 109.
126. D.L. Peng, K. Sumiyama, T. Hihara, S. Yamamuro, T.J. Konno, *Phys. Rev.*, **2000**, *B 61*, 3103.
127. M. Sato, S. Kohiki, Y. Hayakawa, Y. Sonda, T. Babasaki, H. Deguchi, M. Mitome, *J. Appl. Phys.*, **2000**, *88*, 2771.
128. J. Feng, H.C. Zeng, *Chem. Mater.*, **2003**, *15*, 2829.
129. R.H. Kodama, *J. Magn. Magn. Mater.*, **2000**, *221*, 32.
130. V. Biju, A.M. Khadar, *J. Mater. Sci.*, **2003**, *38*, 4005.
131. Z. Fei-bao, Z. Ying-ke, L. Hu-liu, *Mater. Chem. Phys.*, **2004**, *83*, 60.